Journal of Alloys and Compounds 509 (2011) 5887–5892

Contents lists available at ScienceDirect

Journal of Alloys and Compounds

journal homepage: www.elsevier.com/locate/jallcom

The structural and spectroscopic investigations of ternary tellurite glasses, doped with copper

G. Upender*, Ch. Sameera Devi, V. Kamalaker, V. Chandra Mouli

Department of Physics, Osmania University, Hyderabad, 500 007, India

ARTICLE INFO

Article history:
Received 7 July 2010
Received in revised form 2 March 2011
Accepted 2 March 2011

Keywords:
Glassy materials
IR spectroscopy
EPR
Optical absorption

ABSTRACT

Infrared, EPR and optical absorption studies on $(100-2x)TeO_2$–xAg_2O–xWO_3 ($7.5 \leq x \leq 30$) glasses containing Cu^{2+} spin probe have been carried out. The infrared spectral studies show that the structure of glass network consists of $[TeO_4]$, $[TeO_3]/[TeO_{3+1}]$, $[WO_4]$ units in the disordered manner. Physical parameters such as density (ρ), molar volume (V_m), oxygen packing density (OPD), oxygen molar volume (V_O), copper ion concentration (N) and mean copper ion separation (R) have been determined. The spin-Hamiltonian parameters ($g_{||}$, $g_{(}$ and $A_{||}$) of Cu^{2+} ions in the present glasses have been estimated from EPR spectra at 300 K. Bonding parameters such as α^2, β_1^2, β^2, Γ_σ, Γ_π have been calculated from both optical absorption and EPR data. The observed variations in spin-Hamiltonian parameters and bonding parameters have been correlated to the structural modifications due to the WO_3 and Ag_2O incorporation into the TeO_2 glass network.

1. Introduction

Electron paramagnetic resonance (EPR) studies have attracted many researchers because it may provide valuable information related to the structural species of vitreous matrices, due to the great sensitivity of the EPR absorption spectra at symmetry and strength of the ligand field in the neighbourhood of the paramagnetic impurities introduced as a probe. EPR investigations of Cu^{2+} ions in glasses are interesting and have received considerable attention because the EPR parameters of Cu^{2+} are very sensitive to the local symmetry [1–6]. The main advantage of using Cu^{2+} as the spin probe is that its EPR spectra can easily recorded at room temperature, the spectrum is simple and the spread of the spectrum is adequate to detect changes around Cu^{2+} ions in the glass structure. The optical absorption studies on the glassy materials yield important information regarding electronic, vibrational edges, and are also useful in identifying the relevant absorption band position due to transition metal ions. The data obtained from EPR and optical absorption is very much informative about the metal-ligand nature in glasses. There are reports from our laboratory regarding EPR and optical absorption studies of Cu^{2+} ions in tellurite, bismuth and borate based glasses [7–11].

Recently we have published the results on optical band gap, glass transition temperature and Raman studies of TeO_2–Ag_2O–WO_3 glasses [12]. Following the research line of a former work, we have motivated to take up the studies on EPR and optical absorption of TeO_2 glasses containing WO_3 and Ag_2O because a survey of literature indicates that no EPR and optical absorption studies of Cu^{2+} ions doped in TeO_2 glasses containing WO_3 and Ag_2O have been reported so far. In view of the aforementioned aspects, we have carried out EPR, optical absorption and IR studies on copper doped TeO_2–Ag_2O–WO_3 glass system.

The aim of the present paper is to study the short range structure, the effect of heavy metal oxides such as WO_3, Ag_2O on the site symmetries around Cu^{2+} in $(100-2x)TeO_2$–xAg_2O–xWO_3 glass system and to obtain the bonding parameters by correlating EPR and optical absorption data and discuss the variations in these parameters in terms of structural changes of glasses.

2. Experimental

2.1. Glass preparation

1 mol% copper doped glasses in the form of $(100-2x)TeO_2$–xAg_2O–xWO_3 (where $x = 7.5$, 15, 22.5, 30) were prepared by conventional melt quenching technique in the temperature range 750–850 °C depending on the glass composition. The detailed method of preparation is presented elsewhere [12]. The compositions of the glass samples employed in these studies are given in Table 1.

2.2. X-ray diffraction

X-ray diffractograms of powdered glass samples were recorded using a Philips diffractometer of the PANalytical X-pert PRO model with Cu-K_α radiation of wavelength 1.54 Å at room temperature. The obtained XRD patterns of the present glass system showed broad peaks, which are the characteristic peaks of the glass structure for the present glass system.

---

* Corresponding author. Tel.: +91 40 27682242; fax: +91 40 27099020.
E-mail address: upender_b4u@yahoo.co.in (G. Upender).

0925-8388/$ – see front matter © 2011 Elsevier B.V. All rights reserved.
doi:10.1016/j.jallcom.2011.03.001

Table 1
Glass compositions and the IR band positions of the glass system $(100-2x)TeO_2–xAg_2O–xWO_3$.

Sample ID	Composition (mol%)	IR bands (cm^{-1})					
TAW1	$85TeO_2–7.5Ag_2O–7.5WO_3$	460–490	635	658	735	840	924
TAW2	$70TeO_2–15Ag_2O–15WO_3$	460–490	–	666	746	834	918
TAW3	$55TeO_2–22.5Ag_2O–22.5WO_3$	460–490	–	673	764	820	911
TAW4	$40TeO_2–30Ag_2O–30WO_3$	460–490	–	679	775	816	905

2.3. Glass properties

The densities of glasses were determined at room temperature by the Archimedes method using xylene ($\rho = 0.86$ g/cc) as the immersion liquid. Repeated densities measurements were agreed within ±0.01%. From these density values, the molar volume of glasses ($V_m = \Sigma x_i M_i/\rho$) and the molar volume of oxygen (volume of glass in which 1 mol of oxygen is contained, $V_O = (\Sigma x_i M_i/\rho)(1/\Sigma x_i n_i)$) were calculated, here x_i is the molar fraction of each component i, M_i is the molecular weight, ρ is the glass density and n_i is the number of oxygen atoms in each oxide. Oxygen packing density (OPD) of each glass was calculated from the density and composition using the formula $OPD = 1000\,C\,(\rho/M)$, C is the number of oxygens per formula unit. From the measured values of the density (ρ) and average molecular weight, various physical parameters such as copper ion concentration (N), mean copper ion separation (R) are determined and are presented in Table 3.

2.4. IR studies

The IR spectra of the glass samples were recorded at room temperature using a Perkin-Elmer FT-IS spectrometer model 1605 using KBr disc technique. The investigated samples were ground to fine particles and then mixed with KBr in the ratio (0.002:0.2 g) glass to KBr respectively. The weighted mixture was then subjected to a pressure of 5 tons/cm^2. The transmission spectra were measured immediately after preparing the desired disks.

2.5. EPR studies

The room temperature EPR spectra of copper doped glass samples were recorded using JEOL-JM Fe3, EPR spectrometer in the range 220–360 mT operating in the X-band frequency and employing a field modulation of 100 kHz. Polycrystalline diphenyl picryl hydrazyl (DPPH) was used as the standard ‘g’ marker for the determination of the working microwave frequency of EPR spectrometer.

2.6. Optical absorption studies

Optical absorption spectra of all the glass samples (≈1 mm thick) were recorded on a double beam Shimadzu UV-3100 spectrometer in the wavelength range 400–900 nm at room temperature using air as the reference medium. The precision of measuring of wavelength was about ±1 nm. The peak-pick option facilitates to determine exact peak position in the absorption spectrum.

3. Results and discussion

3.1. IR studies

The IR spectra of the $TeO_2–Ag_2O–WO_3$ glasses are shown in Fig. 1. The observed IR band positions for all the compositions are summarized in Table 1. The assignments of IR bands are given in Table 2. The IR spectrum of TAW1 glass consists of six bands at 470, 635, 658, 735, 840 and 924 cm^{-1}. The IR studies on silver tellurite and tungsten tellurite glasses have shown that the observed bands around 635 and 658 cm^{-1} are due to stretching vibrations of Te–O bonds and the band around 470 cm^{-1} is due to stretching vibrations of Te–O–W or bending vibrations of Te–O–Te linkages [13,14]. The observed IR bands at 924 cm^{-1} and a shoulder at 840 cm^{-1} represent the characteristic bands of tungsten glasses which can be attributed to symmetric stretching vibrations of $W–O^-$ and W═O bonds in WO_4 or WO_6 units and stretching vibrations of W–O–W in WO_4 or WO_6 units, respectively [15,16]. As the $WO_3–Ag_2O$ content increases from 15 to 60 mol%, the bands at 635 and 658 cm^{-1} in TAW1 are merged and form a broad band at 666 cm^{-1} and this shifts towards higher wavenumbers: from 666 to 673, and then to 679 cm^{-1}, while the band at 735 cm^{-1} shifts to 746, 764 and then to 775 cm^{-1} (Fig. 1). It is observed from Fig. 2 that as the $WO_3–Ag_2O$ content increases the band at 924 cm^{-1} is shifted to

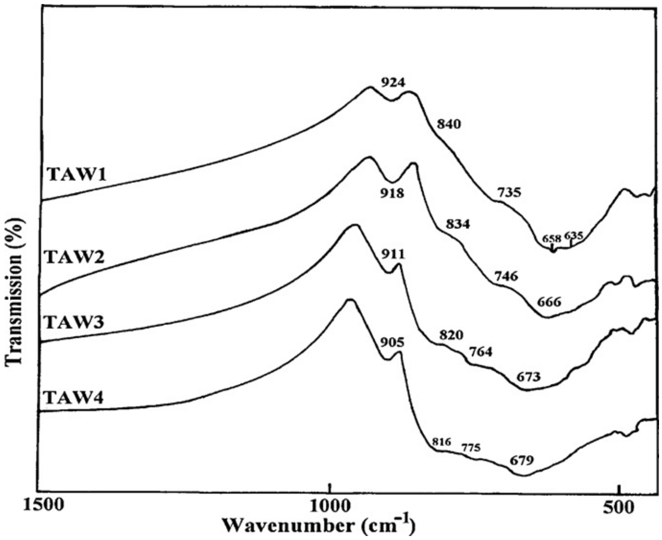

Fig. 1. IR spectra of $TeO_2–Ag_2O–WO_3$ glass system.

Table 2
Assignments of IR bands of glass system $(100-2x)TeO_2–xAg_2O–xWO_3$.

IR band (cm^{-1}) observed in the glass	Assignment
890–930	Stretching vibrations of $W–O^-$ and W═O bonds in WO_4 or WO_6 units
820–850	Stretching vibrations of W–O–W in WO_4 or WO_6 units
600–650	Stretching vibrations of TeO_4 units
730–780	Stretching vibrations of TeO_3/TeO_{3+1} units
650–680	Stretching vibrations of TeO_3 units
460–495	Stretching vibrations of Te–O–W linkages

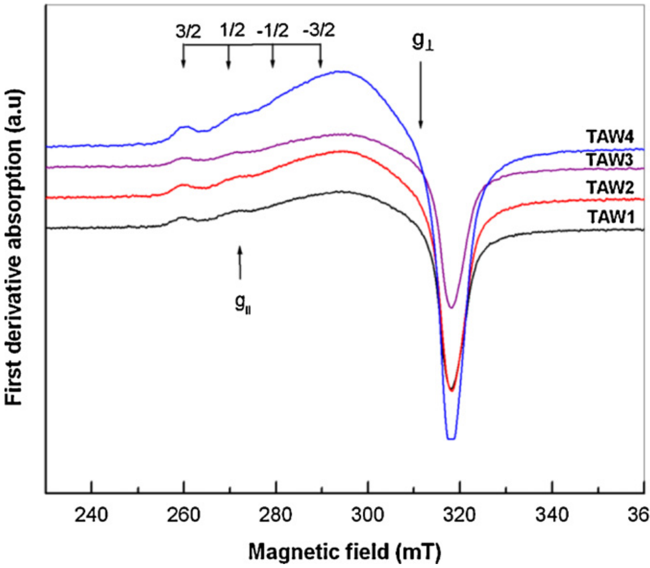

Fig. 2. EPR spectra of Cu^{2+} in $TeO_2–Ag_2O–WO_3$ glass system at room temperature.

Table 3
Physical and optical parameters of Cu^{2+} doped $(100-2x)TeO_2$–xAg_2O–xWO_3 glass system.

Parameter	$x=7.5$	$x=15$	$x=22.5$	$x=30$
Average molecular weight (g/mol)	171.224	182.052	192.881	203.709
Density, ρ (g/cc) (±0.01)	5.965	6.194	6.421	6.655
Molar volume, V_m (cm^3/mol) (±0.1)	28.705	29.392	30.039	30.609
Oxygen packing density (mol/l) (±0.15)	70.023	68.386	66.913	65.667
V_O (cm^3/mol) (±0.05)	14.281	14.623	14.945	15.228
Copper ion concentration, N (×10^{21}/cc)	1.265	1.219	1.205	1.169
Mean copper ion space, R (Å)	9.246	9.361	9.397	9.492
$g_{\parallel}$ (±0.001)	2.352	2.358	2.362	2.357
$g_($ (±0.001)	2.103	2.083	2.088	2.079
$A_{\parallel}$ (×10^{-4} cm^{-1}) (±0.5)	124	113	118	114
λ (nm) (±1)	808	794	805	801
ΔE_{xy} (cm^{-1})	12376	12594	12422	12484
$\Delta E_{xz,yz}$ (cm^{-1})	12662	15801	14878	16624
α^2	0.781	0.746	0.768	0.749
β^2	0.985	1.029	1.002	1.028
β_1^2	0.836	0.904	0.878	0.893
Γ_π (%)	32.79	19.26	24.43	21.39
Γ_σ (%)	47.82	55.04	50.67	54.98

lower wavenumbers: from 924 to 918, 911, and then to 905 cm^{-1}, while the band at 840 cm^{-1} shifts to 834, 820 and then to 816 cm^{-1}. It is also noticeable that band at 470 cm^{-1} is fairly strong for all the samples (TAW1–TAW4). The shifting of the IR bands towards lower or higher wavenumbers and their broadening could be due to the influence of Ag^+ and W^{6+} ions on the tellurite network. The Ag^+ ions break the Te–$_{eq}O_{ax}$–Te bridging bonds forming TeO_2 glass network and form the Te–$_{eq}O^-$–Ag^+ or Te–$_{ax}O^-$–Ag^+ species and also Ag^+ ions break the tungsten network by forming W–O^-–Ag^+ species [13]. The shifting of the IR bands may also be related to the formation of more Te–O–W, W–O–W linkages and W=O, Te=O bonds [13]. All these species converts the TeO_4 units in to TeO_3/TeO_{3+1} units. The formation of Te–O–W linkages is expected because both Te and W atoms have comparable electronegativity values (2.1 and 2, respectively) and can therefore substitute for each other in bonding with oxygen atoms. As the WO_3-Ag_2O content increases, the major band shifts from 658 cm^{-1} (TAW1) to 679 cm^{-1} (TAW4) may be related to the increase of number of TeO_3/TeO_{3+1} units at the expense of number of TeO_4 units.

3.2. *EPR studies*

The origin of EPR spectra of the Cu^{2+} ion in TeO_2 based glasses is found elsewhere [8]. No EPR signal was observed in the spectra of undoped glasses indicating that no paramagnetic impurities were present in the starting materials. The EPR spectra of the TeO_2–Ag_2O–WO_3 glass system doped with Cu^{2+} ions are shown in Fig. 2.

The spectrum closely resembles that of the Cu^{2+} ion in most oxide glasses [17–21]. The EPR spectra of copper ions in all the glass samples have been analyzed using an axial spin-Hamiltonian in which the quadrupole and nuclear Zeeman interaction terms are ignored [22–24].

$$H = g_{||}\beta H_z S_z + g_{\perp}\beta(H_x S_x + H_y S_y) + A_{||}S_z I_z + A_{\perp}(S_x I_x + S_y I_y) \tag{1}$$

Here the symbols have their usual meaning.

The solution of the spin-Hamiltonian gives the expressions for the peak positions related to the principal values of g and A tensor as follows [22–24]:

$$h\nu = g_{||}\beta H_{||} + mA_{||} + \frac{(15/4 - m^2)A_{\perp}^2}{2g_{||}\beta H_{||}} \tag{2}$$

$$h\nu = g_{\perp}\beta H_{\perp} + mA_{\perp} + \frac{(15/4 - m^2)(A_{\perp}^2 + A_{\parallel}^2)}{2g_{\perp}\beta H_{\perp}} \tag{3}$$

for the parallel and perpendicular hyperfine peaks respectively. Here 'm' is the nuclear magnetic quantum number of the copper nucleus with values 3/2, 1/2, −1/2, −3/2 and '(' is the microwave frequency at resonance. Using the Eqs. (2) and (3) the spin-Hamiltonian parameters of all the glasses have been evaluated and are presented in Table 3. The EPR parameters of Cu^{2+} ion in present glasses are compared with other oxide glasses and are in good agreement with earlier reported values [17–21,25–27]. It can be seen from Fig. 2 that when TeO_2 is replaced by WO_3–Ag_2O makes small changes in the shape and position of spectral lines in magnetic field. The addition of WO_3–Ag_2O content results in the marked shift of the lines to higher magnetic fields and intensity of the complete spectrum increases. From Table 3, it is found that $g_{||}$ and $g_($ and $A_{||}$ values change with the composition WO_3–Ag_2O in the present glasses. The composition dependence of $g_{||}$ and $A_{||}$ is shown in Fig. 3. From Table 3 it is clear that $g_{||}$ reaches to a maximum for TAW3, minimum for TAW1 (Fig. 3), $g_($ reaches to a maximum for TAW1, minimum for TAW4 and $A_{||}$ reaches to a maximum for TAW1, minimum for TAW2 (Fig. 3), indicating continuous structural change in the glass system. It also clear from Table 3 that $g_{||}$ value increases with increase of WO_3–Ag_2O content up to 45 mol% and there is considerable decrease in $g_{||}$ with an increase of WO_3–Ag_2O content up to 60%. This indicates that the distortion around Cu^{2+} ion is changing with the increasing WO_3–Ag_2O content. Moreover from Table 3 it is seen that $g_{||} > g_(> g_e$ (where $g_e = 2.0023$ is free electron g-value)

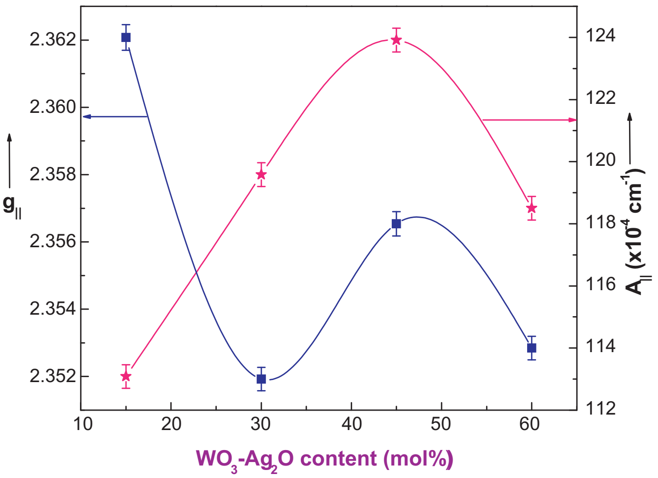

Fig. 3. Variation of $g_{||}$ and $A_{||}$ with WO_3–Ag_2O content.

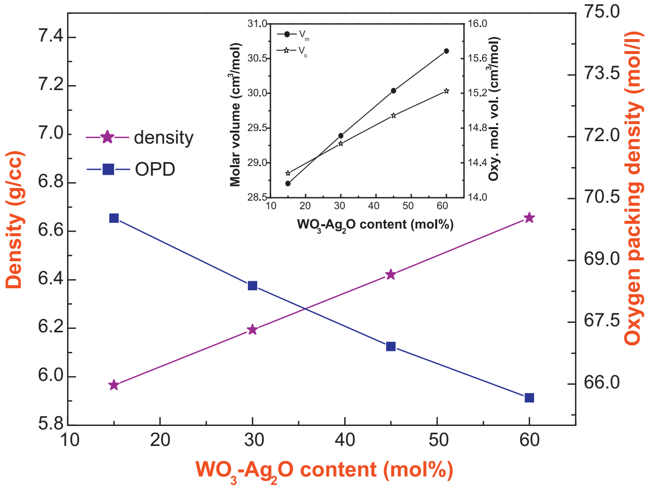

Fig. 4. Compositional variation of density and oxygen packing density. (Inset shows the compositional variation of molar volume and oxygen molar volume.)

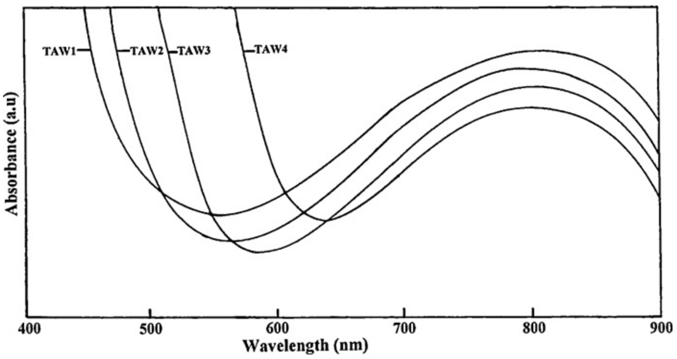

Fig. 5. Optical absorption spectra of Cu^{2+} in TeO_2–Ag_2O–WO_3 glass system.

this suggests that the Cu^{2+} ions in these glasses are coordinated by six ligands (CuO_6 chromophore) which form an octahedron elongated along the z-axis and also suggests that the ground state of Cu^{2+} ions is the $d_{x^2-y^2}$ orbital ($^2B_{1g}$ state) [1,28,29].

The variation in spin-Hamiltonian parameters with increasing WO_3–Ag_2O content is due to structural change in the glass system. This behaviour agrees with the IR spectral studies. The structural variation in glass causes fluctuation in ligand field and in turn, it is reflected in the variation of the spin-Hamiltonian parameters [18,19]. The reasons for the variation in the spin-Hamiltonian parameters can be summarized as follows: when the substitution of TeO_2 mol by mol by WO_3–Ag_2O content, two silver atoms and one tungsten atom ate introduced, while the number of oxygen atoms are same according to the ratio 4/4, this in turn decrease the oxygen packing density from 70.023 to 65.667 mol/l and increase the oxygen molar volume from 14.281 to 15.228 cm^3/mol (see Fig. 4 and Table 3). The large value of the radii (1.26 Å) and bond length (2.54 Å) of Ag_2O compared to those of WO_3 ($r = 0.62$ Å; W–O = 1.90 Å) and TeO_2 ($r = 0.70$ Å; $Te–_{eq}O = 1.99$ Å; $Te–_{ax}O = 2.08$ Å) [13,30] resulted in a formation of excess free volume which increases the overall molar volume (28.705–30.609 cm^3/mol) of these glasses (Table 3); while OPD decrease with increase of WO_3–Ag_2O and therefore the compactness of structural units that surrounds Cu^{2+} ions decreases, due to this the bond length between Cu–O and the interaction between the oxygen and Cu^{2+} may be changed, it causes to vary the ligand field and hence variation in spin-Hamiltonian parameters as observed.

On the other hand the changes in the spin-Hamiltonian parameters with varying modifier content can also be attributed to the change in electron cloud density at the Cu^{2+} ions in the glass network. The change in electron cloud density can be understood in the following way: from the vibrational spectroscopy it is clearly noticed that the addition of modifier content to the TeO_2 network leads to the formation of non-bridging oxygens (NBOs) in the form of $Te–_{eq}O^-Ag^+$, $Te–_{ax}O^-Ag^+$, $W–O^-Ag^+$, $Te–O^-$, Te═O, $W–O^-$ and W═O bonds. Hence the increase in modifier content results in the progressive creation of NBOs at the expense of bridging oxygens (BOs). The NBO which bound an excited electron less tightly than the BO and moreover NBO is more polarizable than the BO. The optical basicity (It is defined as the electron density carried by oxygen and it is represented by 'Λ') of the present glasses may increase with the increase of highly polarizable NBOs. This may be understood according to the relation proposed by Duffy [31].

$$\Lambda = 1.67\left[1 - \frac{1}{\alpha_{O^{2-}}}\right] \tag{4}$$

Here Λ is optical basicity and $\alpha_{O^{2-}}$ is the oxide ion polarizability. This equation shows that with increase in polarizability, the basicity also increases. Therefore the optical basicity of the present glasses increases with an increase in WO_3–Ag_2O content because of more highly polarizable NBOs are present in the glasses with the modifier content. From this observation we can conclude that Cu^{2+} ions are mostly surrounded by NBOs, which may present high electron cloud density at the Cu^{2+} site and hence the variations in spin-Hamiltonian parameters as observed. The variations in EPR parameters not only depend exclusively on the above said reasons but also differences in the field intensities of W^{6+} ions (1.47), Te^{4+} ions (0.71) and Ag^+ ions (0.60) causes the fluctuations in ligand field around Cu^{2+} ions and this in turn vary the spin-Hamiltonian parameters as observed [32].

3.3. Optical absorption studies

The optical absorption spectra of Cu^{2+} doped TAW glasses are shown in Fig. 5 and it shows a single broad absorption whose peak ranges from 794 to 808 nm (12594–12376 cm^{-1}). The Cu^{2+} ion belongs to the $3d^9$ configuration; it has a ground state of ^2D. In a regular octahedral field the ^2D state splits into ^2E_g and $^2T_{2g}$ energy levels. Further ^2E_g level splits into $^2B_{1g}$ and $^2A_{1g}$; and the $^2T_{2g}$ level splits into $^2B_{2g}$ and ^2E_g. Among these, $^2B_{1g}$ will be the ground state. Thus, for copper ions, according to References [33–36] the three bands corresponding to the transitions $^2B_{1g} \rightarrow {}^2A_{1g}$, $^2B_{1g} \rightarrow {}^2B_{2g}$ and $^2B_{1g} \rightarrow {}^2E_g$ are expected. But in the present case, we have observed a single optical absorption band which is in agreement with most of the reports [33–39]. This single optical band was interpreted as the overlap of all the three transitions. Hence in the present paper the observed asymmetric band around 800 nm is assigned to the $^2B_{1g} \rightarrow {}^2B_{2g}$ transition (ΔE_{xy}) of Cu^{2+} ion in octahedral coordination with a strong tetrahedral distortion and the EPR results consistent with this assumption. The absorption peak positions (λ) of present glasses at different concentrations of WO_3–Ag_2O are given in Table 3.

The compositional dependence of optical absorption maxima of the present glasses is shown in Fig. 6. From Fig. 6 it is found that the absorption peak of Cu^{2+} ion in TeO_2–WO_3–Ag_2O glasses is shifted from 808 nm to 794 nm, then to 805 nm and finally to 801 nm with increasing concentration of WO_3–Ag_2O from 15 to 60 mol%. The peak corresponding to Cu^{2+} ion is maximum (808 nm) in $85TeO_2$–$7.5Ag_2O$–$7.5WO_3$. The variation in peak position with WO_3–Ag_2O content indicates the fluctuation in ligand field around the Cu^{2+} probe ion, which is related to change in polarizability of oxygen ions surrounding the Cu^{2+} ion and its dependence on field

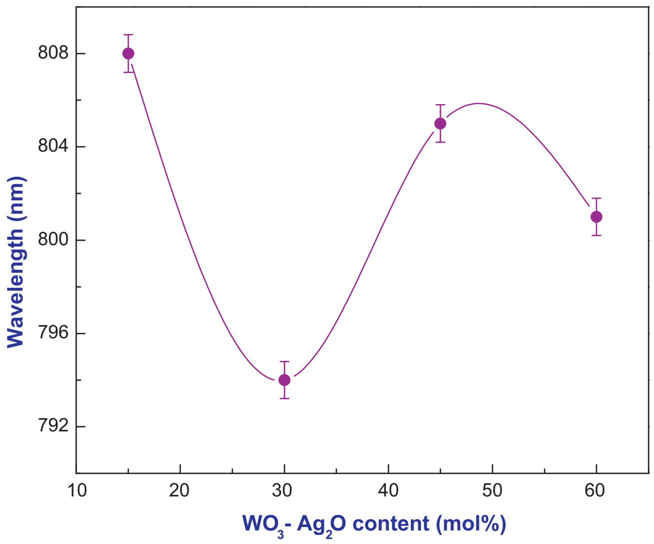

Fig. 6. Variation of optical absorption maxima (λ) with WO_3–Ag_2O content.

strength of Te^{4+} ions (0.71), W^{6+} ions (1.47) and Ag^+ ions (0.60). The change in polarizability of oxygen ions surrounding the Cu^{2+} can be explained as follows. As WO_3–Ag_2O content increases up to 60 mol%, from IR analysis it is observed that mixed Te–O–W and W–O–W linkages are formed, in which the oxygen ions are more polarized than the oxygen ions in Te–O–Te, $Te–O^-Ag^+$, since W^{6+}-ions possess higher field intensity (1.47) than that of Te^{4+}-ions (0.71) and Ag^+ ions (0.60). Therefore this is the reason why the optical absorption maximum varies with Ag_2O–WO_3 content. On the other hand the shift in the optical absorption peak in the present system can be explained on the basis of structural changes take place due to conversion of TeO_4 units into TeO_3/TeO_{3+1} units with WO_3–Ag_2O content.

3.3.1. Cu^{2+}-ligand bond nature

The EPR and optical absorption spectra data can be correlated to understand the environment of Cu^{2+} in TeO_2–Ag_2O–WO_3 glass network, in this connection the bonding parameters or also known as bonding coefficients are evaluated using EPR and optical data by using the following equations [33] and their values are presented in Table 3.

$$g_{||} = 2.0023\left(1 - \frac{4\lambda\alpha^2\beta_1^2}{\Delta E_{xy}}\right) \tag{5}$$

$$g_{\perp} = 2.0023\left(1 - \frac{\lambda\alpha^2\beta^2}{\Delta E_{xy,yz}}\right) \tag{6}$$

where ΔE_{xy} and $\Delta E_{xz,yz}$ are the energies corresponding to the transitions of $^2B_{1g} \rightarrow {}^2B_{2g}$ and $^2B_{1g} \rightarrow {}^2E_g$ respectively, and λ is the spin–orbit coupling constant (=−828 cm^{-1}) [40] and the bonding coefficients α^2, β_1^2 and β^2 (≈1.00) characterize respectively, the in-plane σ bonding with the $d_{x^2-y^2}$ orbital, in-plane (bonding with the d_{xy} orbital and out-of-plane π bonding with the d_{xz} and d_{yz} orbital of the Cu^{2+} complex in the glasses. Their values lie between 0.5 and 1, the limits of pure covalent and pure ionic bonding, respectively [41]. In the present glasses the bonding parameters α^2, β_1^2 and β^2 were evaluated using the following equations [33,42].

$$\alpha^2 = \left|\frac{A_{||}}{P}\right| + (g_{||} - 2) + \frac{3}{7}(g_{\perp} - 2) + 0.04 \tag{7}$$

$$\beta_1^2 = \frac{[(g_{||}/g_e) - 1]\Delta E_{xy}}{4\lambda\alpha^2} \tag{8}$$

$$\beta^2 = \frac{[(g_{\perp}/g_e) - 1]\Delta E_{xy,yz}}{\lambda\alpha^2} \tag{9}$$

Here *P* is dipolar hyperfine coupling parameter (=0.036 cm^{-1}). From the Eqs. (8) and (9), it can be seen that to determine Cu^{2+} bonding coefficients, one needs in addition to the EPR parameters, the energy positions of the absorption bands of Cu^{2+} which indicates the values of ΔE_{xy} and $\Delta E_{xz,yz}$. Since we have observed one absorption band corresponding to $^2B_{1g} \rightarrow {}^2B_{2g}$ transition (ΔE_{xy}, these are presented in Table 3), the position of second band can be estimated by using the following equation [35] and the values are presented in Table 3.

$$\Delta E_{xz,yz}(^2B_{1g} \rightarrow {}^2E_g) = \frac{2K^2\lambda}{2.0023 - g_{\perp}} \tag{10}$$

where K^2 is the orbital reduction factor (K^2 = 0.77) and (is the spin–orbit coupling constant (−828 cm^{-1}).

The normalized covalencies of the Cu^{2+}–O in plane bonding of σ and π symmetry are expressed [33,42] in terms of bonding coefficients α^2 and β_1^2 as follows.

$$\Gamma_\sigma = \frac{200(1 - S)(1 - \alpha^2)}{(1 - 2S)}\% \tag{11}$$

$$\Gamma_\pi = 200(1 - \beta_1^2)\% \tag{12}$$

where *S* is the overlapping integral (S_{oxy} = 0.076). The calculated values of Γ_σ and Γ_π are given in Table 3.

From Table 3, it is observed that the bonding parameters are changing with the composition. The calculated values of $(^2$ for present glasses (0.746–0.781) suggest that the in-plane σ bonding in the glasses is moderately covalent in nature whereas the values of β_1^2 (0.836–0.904) obtained for various glasses indicate that the in-plane π bonding is significantly ionic in nature. The value of β_1^2 depends strongly on network formers and the changes in this parameter can be attributed to the changes in O–X bonds (where X = Te, W) because it reflects the competition in the Cu^{2+}–O–X bonds, between the cupric ion and its neighbouring network former cations X for attracting the lone pairs of the intervening oxygen ions. In the present system the values of β^2 found to be unity and the magnitudes of all bonding parameters are comparable to those found for Cu^{2+} in other glasses [18,39,43,44]. We compared the covalence nature of Cu^{2+}–O bonds in the present tellurite glasses with that of borate glasses and found that the Cu^{2+}–O bonds are less covalent in tellurite glasses than in the borate glasses [18].

4. Conclusions

Transparent and stable glasses were obtained in the Cu^{2+} doped TeO_2–Ag_2O–WO_3 system by melt quenching technique. The density (5.965–6.655 g/cc), molar volume (28.705–30.609 cm^3/mol), oxygen molar volume (14.281–15.228 cm^3/mol) increases while oxygen packing density (70.023–65.667 mol/l) decreases with WO_3–Ag_2O content. From IR results it is found that the addition of WO_3–Ag_2O content to TeO_2 increases the population of lower coordination units [TeO_3]/[TeO_{3+1}] in the glass network at the expense of higher coordination units [TeO_4] and also shows the formation of Te–O–W, $W–O^-Ag^+$, $Te–_{eq}O^-Ag^+$, $Te–_{ax}O^-Ag^+$, Te=O and W=O species in the glass network. For all samples, the EPR absorption spectra are asymmetric, characteristic for Cu^{2+} ($3d^9$) ions in axially distorted octahedral symmetric sites and the ground state of Cu^{2+} is $d_{x^2-y^2}$ orbital ($^2B_{1g}$ state). The values of hyperfine constant and *g* factors reveal the predominantly ionic character of the bonding between copper ions and ligand atoms but the optical absorption results indicate that there is covalency for the in-plane σ-bonding and that the in-plane π-bonding is significantly ionic in nature.

Acknowledgements

One of the authors, Dr. G. Upender is grateful to UGC (University Grants Commission), New Delhi, for providing financial assistance under the scheme of RFSMS (Research Fellowships in Sciences for Meritorious Students). The authors also thank the reviewers for their comments and valuable suggestions.

References

[1] H. Imagawa, Phys. Stat. Sol. B 30 (1968) 469.
[2] H. Hosono, H. Kawazoe, T. Kanazawa, J. Non-Cryst. Solids 34 (1979) 339.
[3] J.M. Dance, J.P. Darnandery, H. Branoby, M. Monveraye, Solid State Commun. 39 (1981) 1999.
[4] N.C. Biswas, R. Dayal, P. Chand, Phys. Chem. Glasses 37 (1996) 31.
[5] R.M. Krishna, J.J. Andre, V.P. Seth, S. Khasa, S.K. Gupta, Opt. Mater. 12 (1999) 47.
[6] V. Ramesh kumar, J.L. Rao, N.O. Gopal, Mater. Res. Bull. 40 (2005) 1256.
[7] S. Suresh, V. Swapna, Chandra Mouli, Ferroelecrics 325 (2005) 105.
[8] G. Upender, G. Vasant, V. Sathe, Chandra Mouli, Phys. Chem. Glasses 50 (2009) 399.
[9] G. Upender, V. Kamalaker, C.P. Vardhani, V. Chandra Mouli, Ind. J. Pure Appl. Phys. 47 (2009) 551.
[10] S. Suresh, J. Chinna Babu, V. Chandra Mouli, Phys. Chem. Glasses 46 (2005) 27.
[11] D. Sreenuvasu, N. Narsimlu, G.S. Sastry, V. Chandra Mouli, J. Mater. Sci. Mater. Elec. 7 (1996) 283.
[12] G. Upender, S. Ramesh, M. Prasad, V.G. Sathe, V.C. Mouli, J. Alloys Compd. 504 (2010) 468.
[13] B.V.R. Chowdari, P. Pramoda Kumari, J. Mater. Sci. 33 (1998) 3591.
[14] S. Rossignol, J.M. Reau, B. Tanguy, J.J. Videau, J. Portier, J. Non-Cryst. Solids 155 (1993) 77.
[15] I. Shaltout, Y. Tang, R. Braunstein, E.E. Shaisha, J. Phys. Chem. Solids 57 (1996) 1223.
[16] P. Charton, L. Gengembre, P. Armand, J. Solid State Chem. 168 (2002) 175.
[17] L.D. Bogomolova, V.A. Jachkin, J. Non-Cryst. Solids 58 (1983) 165.
[18] R.P. Sreekanth Chakradhar, A. Murali, J. Lakshmana Rao, J. Alloys Compd. 265 (1998) 29.
[19] P. Nageswara Rao, B.V. Raghavaiah, D. Krishna Rao, N. Veeraiah, Mater. Chem. Phys. 91 (2005) 381.
[20] G. Lakshminarayana, S. Buddhudu, Spectrochim. Acta Part A 62 (2005) 364.
[21] B.B.Das. Deepa, J. Non-Cryst. Solids 355 (2009) 1663.
[22] A. Abragam, M.H.L. Price, Proc. R. Soc. (Lond.) A 205 (1951) 135.
[23] B. Bleany, Philos. Mag. 42 (1951) 44.
[24] A. Abragam, B. Bleany, EPR of Transition Metal Ions, Clarendon, Oxford, 1970, p. 175.
[25] M. Peteanu, I. Andelean, S. Filip, F. Ciorcas, J. Mater. Sci. Mater. Elec. 7 (1996) 165.
[26] R.V.S.S.N. Ravikumar, R. Komatsu, K. Ikeda, A.V. Chandrasekhar, B.J. Reddy, P.S. Rao, J. Phys. Chem. Solids 64 (2003) 261.
[27] A. Thulasiramudu, S. Buddhudu, J. Quant. Spec. Rad. Trans. 97 (2006) 181.
[28] L.D. Bogomolova, Y.G. Tepliakov, F. Caccarale, J. Non-Cryst. Solids 194 (1996) 291.
[29] I. Ardelean, M. Peteanu, S. Filip, V. Simon, G. Guosffy, Solid State Commun. 101 (1997) 341.
[30] R.C. West, M.J. Astle, W.H. Beyer (Eds.), Handbook of Chemistry and Physics, CRC, Boca Raton, FL, Section F-157, 1987.
[31] J.A. Duffy, Phys. Chem. Glasses 30 (1989) 1.
[32] D. Munoz-Martin, M.A. Villegas, J. Gonzalo, J.M. Fernandez-Navarro, J. Eur. Ceram. Soc. 29 (2009) 2903.
[33] D. Kivelson, R. Neiman, J. Chem. Phys. 35 (1961) 145.
[34] I. Siegel, J.A. Lorence, J. Chem. Phys. 45 (1966) 2315.
[35] A. Klonkowski, Phys. Chem. Glasses 24 (1983) 166.
[36] J.M. Duran, Farnandez Navarro, Phys. Chem. Glasses 26 (1985) 26.
[37] R.M. Krishna, J.J. Andre, R.P. Pant, V.P. Seth, J. Non-Cryst. Solids 232–234 (1998) 509.
[38] G. Ramadevudu, Md. Shareefuddin, N. Sunitha Bai, M.L. Rao, M.N. Chary, J. Non-Cryst. Solids 278 (2000) 205.
[39] R.P. Sreekanth Chakradhar, B. Yasoda, J.L. Rao, N.O. Gopal, J. Non-Cryst. Solids 352 (2006) 3864.
[40] F.M. Mabbs, D. Machin, J. Magnetism and Transition Metal Complexes, Chapman and Hall, London, 1973, P154.
[41] R.H. Sands, Phys. Rev 99 (1955) 1222.
[42] H.A. Kuska, M.J. Rogers, R.E. Durllinger, J. Phys. Chem. 71 (1967) 109.
[43] B. Karthikeyan, S. Mohan, Mater. Lett. 57 (2003) 3789.
[44] J. Lakshmana Rao, G. Sivaramaiah, N.O. Gopal, Phys. B: Cond. Mat. 349 (2004) 206.